Computational and Structural Biotechnology Journal 19 (2021) 4997–5007

COMPUTATIONAL AND STRUCTURAL BIOTECHNOLOGY JOURNAL

journal homepage: www.elsevier.com/locate/csbj

A quantitative systems pharmacology model for acute viral hepatitis B

Eduardo Asín-Prieto [a,b,1,2], Zinnia P. Parra-Guillen [a,b,1], José David Gómez Mantilla [a,b,3], Joris Vandenbossche [c], Kim Stuyckens [c], Xavier Woot de Trixhe [c], Juan José Perez-Ruixo [c], Iñaki F. Troconiz [a,b,*]

[a] Pharmacometrics & Systems Pharmacology Lab, Department of Pharmaceutical Technology and Chemistry, School of Pharmacy and Nutrition, C/Irunlarrea 1, University of Navarra, Pamplona 31080, Spain
[b] IdiSNA, Navarra Institute for Health Research, C/Irunlarrea 3, 31008 Pamplona, Spain
[c] Global Clinical Pharmacology, Janssen Research & Development, Turnhoutseweg 30, 2340 Beerse, Belgium

ARTICLE INFO

Article history:
Received 3 June 2021
Received in revised form 31 August 2021
Accepted 31 August 2021
Available online 02 September 2021

Keywords:
Hepatitis B
Quantitative systems pharmacology
Mechanistic modeling
Immune system dynamics
Viral dynamics

ABSTRACT

Hepatitis B liver infection is caused by hepatitis B virus (HBV) and represents a major global disease problem when it becomes chronic, as is the case for 80–90% of vertical or early life infections. However, in the vast majority (>95%) of adult exposures, the infected individuals are capable of mounting an effective immune response leading to infection resolution. A good understanding of HBV dynamics and the interaction between the virus and immune system during acute infection represents an essential step to characterize and understand the key biological processes involved in disease resolution, which may help to identify potential interventions to prevent chronic hepatitis B.

In this work, a quantitative systems pharmacology model for acute hepatitis B characterizing viral dynamics and the main components of the innate, adaptive, and tolerant immune response has been successfully developed. To do so, information from multiple sources and across different organization levels has been integrated in a common mechanistic framework. The final model adequately describes the chronology and plausibility of an HBV-triggered immune response, as well as clinical data from acute patients reported in the literature. Given the holistic nature of the framework, the model can be used to illustrate the relevance of the different immune pathways and biological processes to ultimate response, observing the negligible contribution of the innate response and the key contribution of the cellular response on viral clearance. More specifically, moderate reductions of the proliferation of activated cytotoxic CD8+ lymphocytes or increased immunoregulatory effects can drive the system towards chronicity.

Abbreviations: AHB, acute hepatitis B; ALT, alanine aminotransferase; anti-HBc, specific antibodies against core hepatitis B antigen; anti-HBs, specific antibodies against surface hepatitis B antigen; CHB, chronic hepatitis B; CTL, antigen-specific cytotoxic T lymphocytes; CTL*, activated CTL; CTLm, memory CTL; DC, dendritic cells; DC*, activated dendritic cells; dHep, debris hepatocytes; HB, Hepatitis B; HBsAg, hepatitis B surface antigen; HBV, hepatitis B virus, HBV DNA, circulating DNA levels of HBV; Hep, hepatocytes; Hep_{tot}, total hepatocytes; iHep, infected hepatocytes; IFN, interferon; LN, lymph node; LPC, long-lived plasma cells; LV, liver; MDSC, myeloid-derived suppressor cells; NK, natural killer cells; NK*, activated NK; ODE, ordinary differential equations; PB, plasmablasts; PC, plasma cells; pDC, plasmacytoid DC; PL, plasma; SPC, short-lived plasma cells; QSP, quantitative systems pharmacology; Th0, naïve T cells; TRAIL, tumor necrosis factor–related apoptosis-inducing ligand; Treg, regulatory T cells.

* Corresponding author at: Pharmacometrics & Systems Pharmacology Research Unit, Department of Pharmaceutical Technology and Chemistry, School of Pharmacy and Nutrition, University of Navarra, C/Irunlarrea 1, 31080 Pamplona, Spain.
E-mail address: itroconiz@unav.es (I.F. Troconiz).
[1] These authors share first authorship.
[2] Present address: PharmaMar, Avda. De los Reyes, 1, Pol. Ind. La Mina-Norte, Colmenar Viejo, 28770, Madrid, Spain.
[3] Present address: Boehringer Ingelheim Pharma GmbH & Co. KG, Birkendorfer Str. 65, 88397 Biberach an der Riß, Germany.

https://doi.org/10.1016/j.csbj.2021.08.052

1. Introduction

Hepatitis B is a liver infection caused by the hepatitis B virus (HBV). Upon infection, HBV can trigger an acute response leading to infection resolution (AHB), but the disease can also progress to a chronic state (CHB). Currently, it is estimated that more than 240 million individuals are chronically infected worldwide and between 15% and 40% of this infected population will developed complications such as cirrhosis or hepatocellular carcinoma, and eventually will die [1]. In 2015, CHB resulted in 887,000 deaths worldwide [2], representing a major global health problem.

Despite the large number of treatments for HBV, such as antiretroviral nucleos(t)ide analogs or immunomodulators, complete eradication of the virus from the system (i.e., virologic cure) is currently unattainable, with functional cure (i.e., sustained loss of hepatitis B surface antigen, HBsAg, and HBV DNA in serum) being the main clinical goal [3]. In this regard, the rate of functional cure (i.e., loss of hepatitis B surface antigen [HBsAg]) of approved treatments is below 11% in best case scenarios [1,4], thus justifying current drug development programs. Although additional research is still needed, promising results are being obtained when incorporating novel agents, such as nucleic acid polymers, to current therapeutic strategies [5,6].

HBV infection is a highly complex disease triggering multibranched immune mechanisms, several of them still controversial. Very briefly, the virus is sensed by the innate immune machinery and can trigger an antiviral response [7,8]. This response could be downregulated by the virus through different mechanisms, thus appearing as a "stealth virus" [9,10]. On the other hand, the cellular response has been largely postulated to be responsible for viral clearance through cytolytic and non-cytolytic mechanisms [11,12], leading to a prolonged and polyclonal CD8+ T cell response in patients recovering from the disease. Finally, the humoral response is involved in the clearance of circulating viral particles as well as the prevention of viral spread [13], although its relative contribution to viral control is unclear. In certain cases, an immuno-tolerant response capable of limiting the effector immune response can be triggered due to the immunologic nature of the liver. This regulatory response has been postulated as one of the drivers of HBV chronicity [14,15]. The underlying immune processes involved in development of CHB are not completely understood [16], it is clear that a mature immune system leads to AHB with a potent and effective immune response and, eventually, resolution of >95% of cases in adults, while neonatal and infant infection (e.g., vertical transmission) leads to chronicity 80–90% of the time [2]. Thus, the likelihood of progression from acute to chronic infection highly depends upon the infection age.

Under this complex dynamic scenario, several mathematical models have been developed to understand quantitatively the interplay between viral dynamics, including HBV, and the immune response. These models typically account for the time course of healthy and infected hepatocytes, viral particles, and some type of effector cells and/or cytokines in a semi-mechanistic fashion [17–24]. The major limitation of these models lies in the oversimplification of the immune components, thus reducing their utility to explore the role of each component of the immune system in the final response.

Due to the complexity and fast evolving knowledge of the immune system, as well as the difficulty in parametrizing such big networks, examples of this kind of model are scarce. One of the most relevant efforts was made by Marchuk et al. [25], who developed a model in 1991 to describe and simulate the viral dynamics of AHB infection, including a full immune response. Nevertheless, this model failed to describe immune tolerance mechanisms (some of them discovered after the development of the model), was based on animal data (whose immune physiologic pathways differed compared with humans and cannot completely recapitulate HBV replication), and also lacked compartmentalization (description of the biological entities across the main physiologic compartments). A relevant example that considers this aspect of compartmentalization, although not applied to HB, is the model developed by Palsson et al. [26] for tuberculosis.

Recently, a topological representation characterizing the known interactions between the key elements of the HBV and the immune system–in terms of location, causality, and the nature of the relationship–was developed by our group [27]. Although this representation does not account for the magnitude, breadth, nor the temporality of the response, it provides a comprehensive overview of the system that can inform the building of a comprehensive quantitative system pharmacology (QSP) model. Consequently, and using the above-mentioned topological representation as the starting point, the objective of this work was to develop a multiscale QSP model that is able to characterize mechanistically the dynamics and role of the different components of the immune system at a cellular level during an acute response against HBV, the potential drivers of HB chronicity. The model could potentially be used as a platform to evaluate pharmacologic targets.

2. Mathematical modeling

2.1. Description of the mathematical model

Focusing model scope on acute HBV response characterization, the mathematical model structure proposed here is based on the comprehensive literature review and previously published topological representation [27]. This topological network proposes the interaction between the virus and key players of the innate, adaptive, and immunoregulatory system across 3 relevant compartments: liver (LV), plasma (PL) and lymph node (LN).

A brief overview of the dynamic of the different system components, as well as their effects, implemented in the final mathematical model is provided below. Fig. 1 schematically represents the structure of the model showing the elements and the relationships described below.

2.1.1. Viral dynamics

The model assumes that the system is initiated with a viral load arriving to the liver. After viral inoculation, HBV can infect healthy hepatocytes (Hep) and be cleared or be distributed through plasma. In turn, infected hepatocytes (iHep) can produce more virus, but also HBsAg that can also be distributed to plasma. All hepatocytes (healthy and infected) are subject to natural death, thus producing debris hepatocytes (dHep), responsible for the production of the hepatic damage biomarker alanine aminotransferase (ALT). Given that HBV is not considered a cytopathic virus and that the number of total hepatocytes (Hep_{tot}) is not expected to significantly vary during the acute setting, a quick equilibrium between hepatocyte death and generation was assumed, thus Hep is the difference between total and infected hepatocytes.

2.1.2. Innate response

To characterize the innate response, a pool of naïve dendritic cells (DC) and natural killer (NK) cells with a zero-order synthesis rate in plasma, which accounts for bone marrow formation, and distribution from plasma to liver, was assumed. Upon virus recognition, liver DC are then activated (DC*). A fraction of these DC*, representing plasmacytoid DCs (pDC), produce interferon α (IFNα), a cytokine known to inhibit viral replication as well as promote NK cell activation (NK*). Similar to DC*, NK* cells produce IFNγ, which can also inhibit viral replication. In addition, a fraction of these

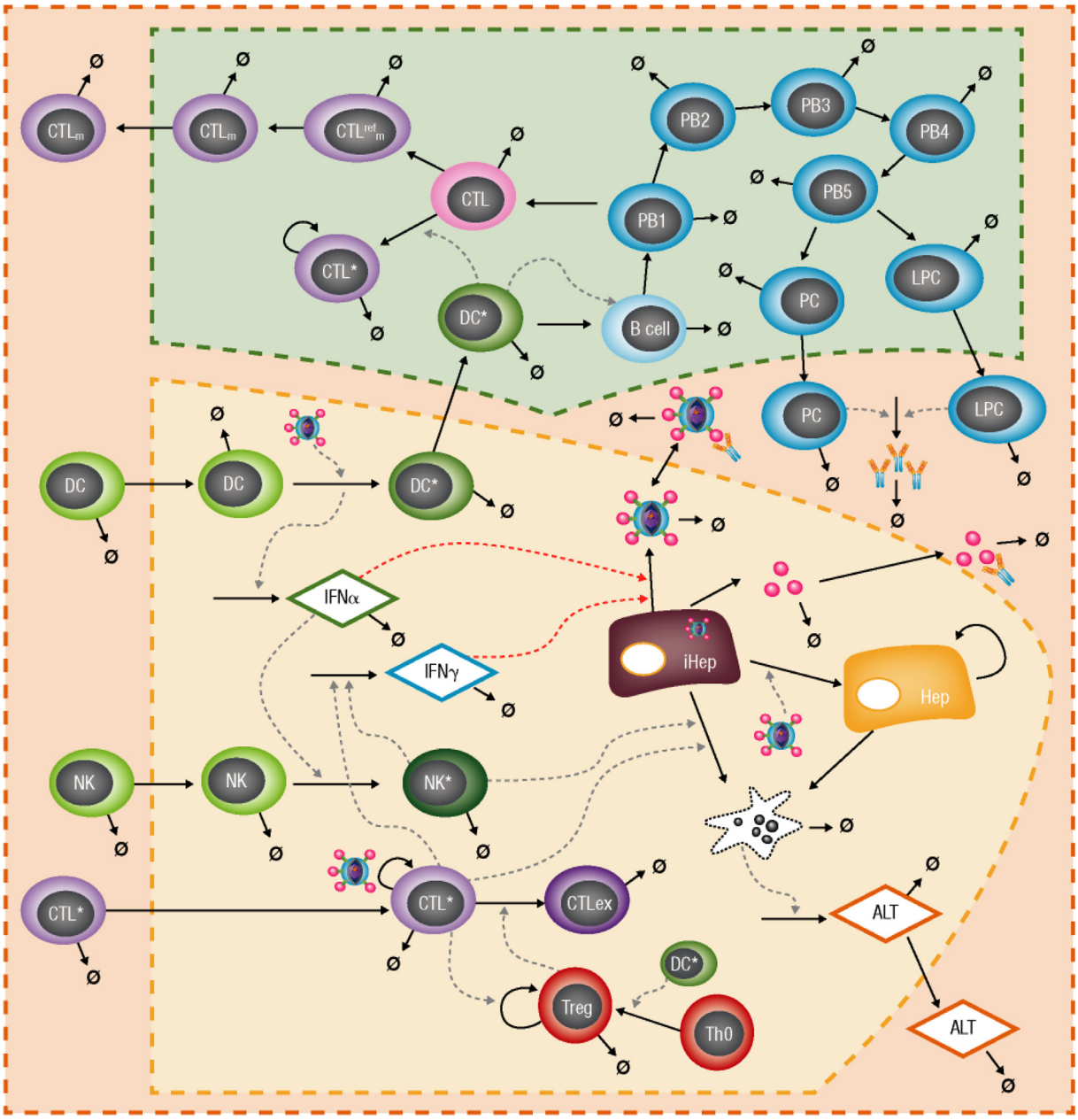

Fig. 1. Schematic representation of the quantitative systems pharmacology model. Model developed across 3 compartments: liver (yellow), lymph (green) and plasma (orange). Entities described within the text. Solid lines indicate processes of synthesis, degradation or transport that impact on entities levels, dotted lines indicate stimulatory (grey) or inhibitory (red) effects. (For interpretation of the references to colour in this figure legend, the reader is referred to the web version of this article.)

NK*, accounting for NK cells expressing TRAIL, is also able to induce direct iHep death.

On the other hand, a decrease in IFNα synthesis, triggered by HBsAg, is implemented in the model to acknowledge the capability of the virus to limit the innate response against HBV.

2.1.3. Adaptive response

DC* act as the link between innate and adaptive response by triggering cellular and humoral events. In the case of the cellular response, DC* can migrate directly from liver to lymph tissues, where they trigger the activation and recruitment process of naïve CD8+ T cells to become CD8+ antigen-specific cytotoxic T lymphocytes (CTL). Upon antigen presentation by DC* to CTL, HBV-specific CTL (CTL*) are generated. These CTL* distribute from lymph node, through plasma to the liver where they exert a non-cytotoxic antiviral activity via the production of IFNγ, as well as a direct cytotoxic activity killing iHep. Both lymphatic and liver CTL* are considered to be capable of self-proliferation up to a maximum level as long as there is viral presentation or viral load. A fraction of the lymph-generated CTL* can evolve to memory CTL (CTLm).

In addition to the cellular adaptive response, the model also accounts for the HBV-specific humoral response. The presence of DC* in the lymph node triggers the activation of an existing pool of naïve B cells, which will then convert to plasmablasts (PB) and initiate a maturation process, until plasma cells (PC) are obtained. Two populations of PC were considered in the model-short-lived PC (SPC) and long-lived PC (LPC)- to enable for a sustained antibody response. Both PC can then distribute to plasma where they produce specific surface antibodies (anti-HBs) that increase the

clearance of HBsAg and viral particles (HBV), as well as antibodies against core antigen (anti-HBc).

The time course of CD4+ lymphocytes was not explicitly included in the model despite their regulator role of effector response, as they were not considered a limiting factor of the immune response in this specific disease.

2.1.4. Immunotolerant response

Given the immune tolerogenic nature of the liver, DC* can activate the generation of liver regulatory T cells (Treg), differentiating from a liver pool of naïve T cells (Th0) in order to control the immune response. Treg can self-proliferate as long as a cellular response (CTL*) is still present, and limit liver cellular response upon the induction of CTL exhaustion.

Myeloid-derived suppressor cells (MDSC) were not included at this stage given the scope of the model and the limited information available from a modeling perspective during the acute phase of hepatitis B. Therefore, assuming that Treg represent both immunotolerant effects.

2.2. Model building

Ordinary differential equations (ODEs) were used to describe the time course of the system components across the 3 identified compartments: LV, PL, and LN. In general, synthesis characterized by k_{syn} rate constants was implemented for all components except for infected hepatocytes, for which infection was considered and modeled through a k_{inf} rate constant. Similarly, degradation or death, controlled by k_{deg} and k_{death} rate constants, were specified for all molecular and cellular components, respectively. In addition, activation, exhaustion, or lytic processes represented by k_{act}, k_{exh}, and k_{lytic} rate constants were considered. Finally, distribution between compartments was also accounted for when biologically needed (e.g., DC* distribute to lymphoid tissue to active CD8+ cells, and these activated CD8+ reach the liver through the blood stream).

The different biological processes previously detailed (e.g., synthesis, degradation, distribution) were implemented using zero-, first- or second-order rate constants. Michaelis-Menten or Hill kinetic functions were also implemented to account for saturation processes.

The equation below, which describes the temporal course of iHep, is provided as an example.

$$\frac{diHep}{dt} = k_{inf} \times HBV_{LV} \times Hep - k_{death_{Hep}} \times iHep - k_{lytic\_CTL} \times CTL^{*} \times iHep - k_{lytic\_NK} \times NK^{TRAIL} \times iHep$$

The complete set of equations can be found in the Supplementary Appendix 1. The final model accounted for a total of 32 biological entities across ≥ 1 compartment, described through 41 ODEs and 6 analytical equations. Note that due to data limitations, proportionality was assumed across some entities if specific rates were not required (e.g., IFNs in plasma–potentially useful biomarkers–were assumed to reflect liver quantities after volume correction). Viral replication was considered negligible when < 1 hepatocyte was infected.

Mathematical equations were implemented and the dynamics of the different components were simulated using the Simbiology® toolbox from Matlab® (R2019a).

2.3. Model parametrization and initial conditions

Several methods were applied to provide adequate initial conditions for model entities and parameter estimates for the reactions (n = 103). We can differentiate between 2 types of parameters: those that reflect physiological conditions (e.g., organ volumes or entity levels at baseline) and those parameters describing the rate of the different biological and disease processes. Below, the different methods are described with the associated assumptions and the degree of uncertainty. A special effort was made to avoid data not coming from human origin and to select mechanistic and robust data from the literature.

1. Physiological values extracted directly from the literature: This methodology was primarily used for estimates or parameters that were well established and assumed to be physiologically plausible. As an example, the liver volume was set to 1500 mL, rounding the value provided by Herman [28] (1470 cm^3).
2. Physiological values calculated from published information: Data were obtained from 1 or more sources and used for the derivation of the parameters. One example is the derivation of the volume of plasma in the body, assuming that around 60% of the total blood volume (ca. 5 L) corresponds to plasma, leading to a derived plasma volume of 3000 mL [29]. In another example, the number of Hep_{tot} was derived assuming that the hepatic volume is 1470 cm^3 [28], the volume of a single hepatocyte is 4900 μm^3 [30], and the parenchymal cell percentage of the total liver is 80%. The total hepatocyte cell number was estimated to be 2.4×10^{11} cells.

$$Hep_{tot} = \frac{1470cm^3 \times 0.8 \times 10^{12} \frac{\mu m^3}{cm^3}}{4900 \frac{\mu m^3}{cell}} = 2.4 \times 10^{11} cells$$

3. Derived parameters or initial conditions from the implemented QSP model: Some of the parameters were directly derived from model equations to ensure homeostasis in the absence of viral infection. This was the case for the daily production of naïve DCs or NK cells in plasma.
4. Reused model parameter estimates from previously published models: In these cases, the estimates were obtained from previously published theoretical or applied models. Special attention was paid to evaluate the model assumptions and the nature of the data or references used for model development. When available, >1 reference was consulted to increase confidence in the parameter value. As an example, the infection rate constant was obtained from a previous model fitted to clinical data from hepatitis B infected patients under treatment [19]. This model included uninfected and infected hepatocytes and the virus. The infection rate constant was estimated 3×10^{10} mL/(virion*day) (ranging from 0.7×10^{10} to 6.7×10^{10}). Similarly, other authors used a value for the infection rate constant within the same range (4×10^{10} mL/[virion*day]) when fitting data from patients under treatment and modelling uninfected and infected hepatocytes, viruses, and effector cells [31].
5. Parameter estimation from literature experimental data: When parameterization of the biological processes was not directly available, but experimental data quantitatively characterizing the individual process (commonly through in vitro designs) was identified, data from the original publication was extracted or digitalized using WebPlotDigitizer 3.8 and fitted to a model, as previously shown [32]. For example, this approach was used to identify the IFNγ liver concentration inhibiting 50% of HBV synthesis ($IFN\gamma_{50\_HBV}$) based on experimental data from 2 publications [33,34], where the inhibition of HBV replication in a liver cell line was explored in vitro at different IFNγ levels

and under different conditions. The inhibitory model developed was further challenged using additional validation data corroborating the noncytolytic effect of IFNγ on viral replication [35].

6. Calibrated parameters: Unfortunately, quantitative information to characterize all described biological interactions was not available. In those situations, arbitrary values (n = 6) or fine-tune estimates (n = 4) within plausible ranges were used to achieve a desired behaviour. For example, Hill functions were implemented on some processes to act like enablers, activating or deactivating certain processes in the presence or absence of a minimum level of a second component (e.g., activation of DCs in the presence of viral levels). The implications of these estimates in model performance were later explored through sensitivity analyses (see below).

In Table S1, all 103 parameters used in the model are listed along with their value and range if available, the methodology used for their extraction, and the references.

2.4. Model evaluation

Model performance was evaluated at 2 levels. First, the capability of the model to reproduce the temporal and sequential appearance of the different entities in a biological and plausible manner was evaluated and compared to general disease progression knowledge. Then, typical (median) model predictions were compared to clinical data extracted from 4 publications where the time course of different biological markers in acute patients was reported. These biological markers included HBV DNA circulating levels, as well as ALT, HBsAg activated CTL, or IFNα levels in plasma. Data were digitalized from original figures using WebPlotDigitizer 3.8. An overview of the clinical studies can be found in Table 1. To compare model predictions to observed data, time profiles were normalized with respect to HBV DNA peak, as infection time is unknown in most real cases.

2.5. Parameter analyses

Robustness of the final model and impact of the different implemented processes on model entities was assessed through a local sensitivity analysis using the complex-step approximation method (MATLAB, R2019a). The fully normalized sensitivity profiles over time for all the model components were computed and the integral was reported.

In addition, a parameter scan analysis was performed to assess the impact of individual parameter variations (+/- 50%) on relevant end points and identify those processes that could drive the system towards a chronic infection situation. Infection resolution was considered if plasma HBV DNA levels fell below 20 IU/mL (i.e. undetectable levels) and change in time to resolution was computed taking into consideration the maximum simulation time of 45 weeks.

2.6. Exploring model behaviour

2.6.1. Relevance of immune pathways.

A "knock-out" analysis was performed to evaluate the relative importance of the innate (k_{act_NK} = 0 or k_{act_DC} = 0), cellular (k_{act_CTL} = 0) or humoral (k_{act_Bcell} = 0) immune response components on the profile of HBV DNA, the main marker of adequate clearance of the infection. The role of the immunoregulatory response was also explored by modifying the sensitivity of regulatory cells proliferation to CTL presence ($CTL_{50\_Treg\_prol}$) or the inhibitory effect of regulatory cells on CTL response ($Treg_{50\_Treg\_exh}$).

2.6.2. Chronicity

The capability of the model to mimic acute status or development of chronicity was evaluated at a population level computing the percentage of subjects self-resolving the disease (i.e., HBV DNA < 20 IU/mL at week 45). To do so, a virtual population (n = 500) was generated assuming a log normal distribution with 30% variability of the most influential parameters identified during a parameter scan (sensitivity index above 50 units). The distributions were truncated to limit the simulated values to the reported ranges for the different model parameters (Table S1). The process was repeated 100 times to obtain a confidence interval around the percentage of self-resolving patients.

3. Results

The final HBV model comprised a total of 41 ODEs and 6 analytical equations defined by 84 parameters to enable the prediction of the time course of main viral and liver components, as well as cellular and molecular entities of the innate and adaptive response

Table 1
Overview of clinical data studies used for model evaluation.

Reference	Brief description	Measured variables
Webster 2000 [58]	5 patients identified during incubation period Day 0 based on the most recent possible time point of infection	• HBV DNA (pg/mL) (n = 5) • ALT (U/L) (n = 5) • HBsAg (boolean) (n = 5) • IgM anti-HBc (Boolean) (n = 5) • NK cells (cells/mL) (n = 3) • HBV-specific CD8+ (cells/mL) (n = 3)
Dunn 2009 [46]	21 patients with acute HBV sampled during pre-symptomatic phase Day 0 on first symptomatic day	• HBV DNA (IU/mL) (n = 9) • ALT (IU/L) (n = 8) • HBsAg (boolean) (n = 6) • IgM anti-HBc (Boolean) (n = 5) • IFNa (pg/mL) (n = 3) • HBV-specific CD8+ (cells/mL) (n = 4)
Fisicaro 2009 [45]	2 blood donors found to have seroconverted during virological screening every 3 months Day 0 assumed at previous serological screening day	• HBV DNA (IU/mL) (n = 2) • ALT (IU/L) (n = 2) • HBsAg (boolean) (n = 2) • anti-HBs (U/L) (n = 2) • anti-HBc (Boolean) (n = 2)
Chulanov 2003 [37]	21 patients hospitalized with suspected acute viral hepatitis and confirmed of HBV monoinfection Day 0 based on first symptomatic (illness) day	• HBV DNA (ge/mL) (n = 21) • ALT (ULN) (n = 21) • HBsAg (μg/mL) (n = 21)

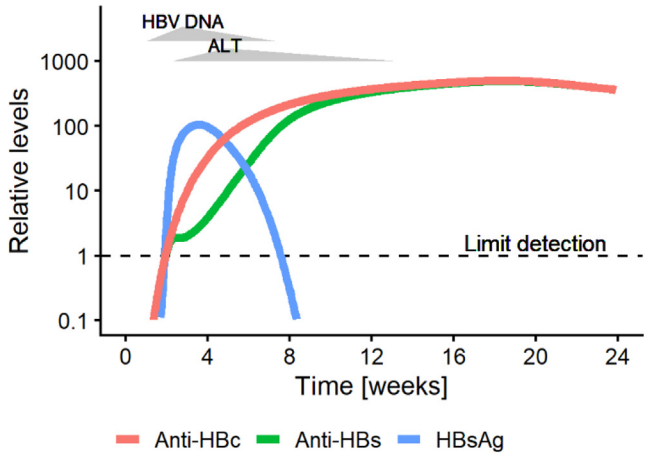

Fig. 2. Disease course of AHB. Model predicted time course of common biomarkers of AHB disease normalized to their limit of detection. For HBV DNA and ALT triangles represent the span and the time of peak levels. Entities defined within the text.

across 3 compartments: liver, plasma and lymph tissue (Supplementary Fig. 1).

3.1. Model evaluation

The model was capable of reproducing the general knowledge regarding the typical time course of the acute disease in patients as shown in Fig. 2. Although a quick disease onset of 3 weeks was predicted after viral infection, the model predicted that viral levels < 200 IU/mL would be reached 52 days after viral peak, and complete viral eradication (<20 IU/mL) in approximately 8 weeks. Similarly, peak in ALT levels is predicted 2 weeks after HBV DNA peak, and 3 weeks after the appearance of detectable HBsAg (>0.1 ng/mL). Levels of HBsAg remain above the cut-off for up to 10 weeks after inoculation. Antibody response was predicted to be delayed on infection, with anti-HBs levels arising above the protection threshold (10 IU/mL) between weeks 7–8 after infection, once HBsAg levels are undetectable.

Moreover, the proposed model was able to capture the time course of relevant clinical biomarkers from patients with acute HBV infection extracted from several publications, as shown in Fig. 3. To note, only ALT levels extracted from clinical data were used to calibrate ALT-related model parameters using the final model structure; the rest of the clinical data were used as a validation set.

3.2. Parameter analyses

Results from the local sensitivity analysis are presented in Fig. 4. Parameters governing the proliferation/death of CTL, followed by those directly affecting viral dynamics (infectivity, target cells, and viral synthesis) and the parameters regulating the appearance of PC (mean transit time and number of transits of PB) were the most influential on HBV levels.

To evaluate the impact of the above processes not only on the time course of hepatitis B infection, but also the probability of becoming chronic (i.e., time to cure), a parameter scan was performed. The 20 most influential parameters on peak viral levels and time to cure are shown in Fig. 5A. The processes influencing peak or area under the curve levels (not shown) are in close agreement to those identified in sensitivity analysis. However, under the acute scenario, only the change in the proliferation capability of T cells was able to switch from responder to non-responder, while moderate changes in the rest of meaningful parameters such as viral replication capability (k_{syn_HBV}) impact the maximum levels or time to cure, but not the ultimate response (Fig. 5B).

3.3. Exploring model behaviour

3.3.1. Contribution of immune pathways

The relative contribution of each of the implemented pathways on the time profile of relevant disease biomarkers – viral load, HBV antigens, and ALT- was explored by individually suppressing or activating their triggers one at a time (Fig. 6).

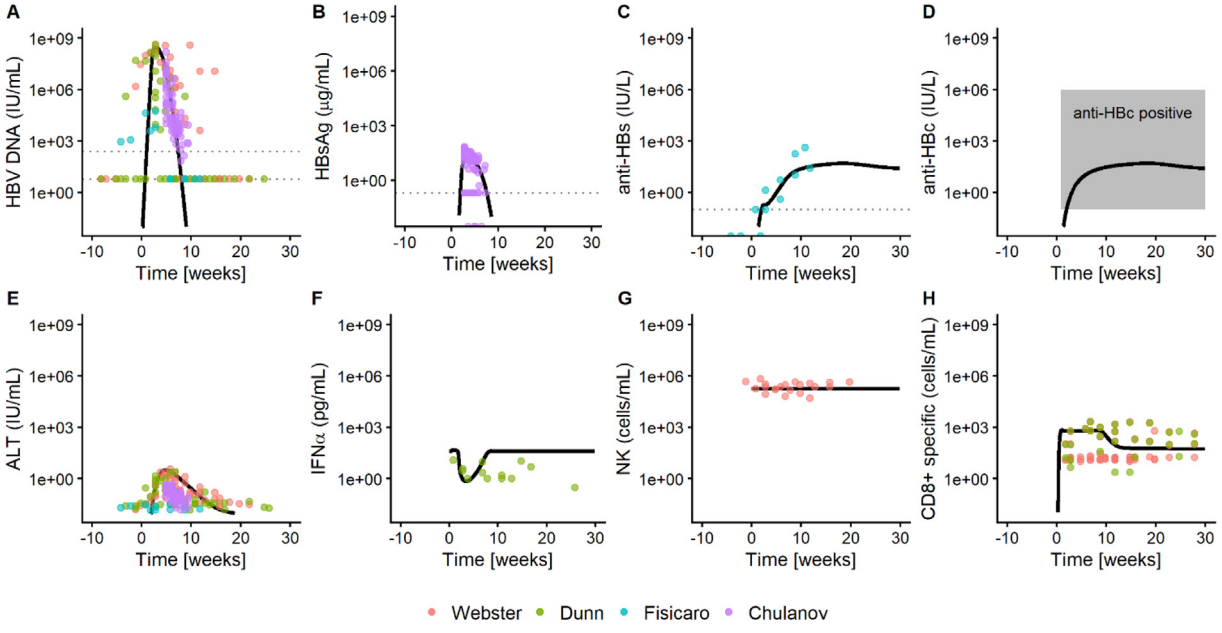

Fig. 3. Evaluation of the final AHB model. Model predictions (solid line) versus real data (points) extracted from 4 different clinical studies: Webster et al. [58], Dunn et al. [46], Fisicaro et al. [45], and Chulanov et al. [37]. See Table 1 for further details on data availability and study characteristics. Model entities defined within the text.

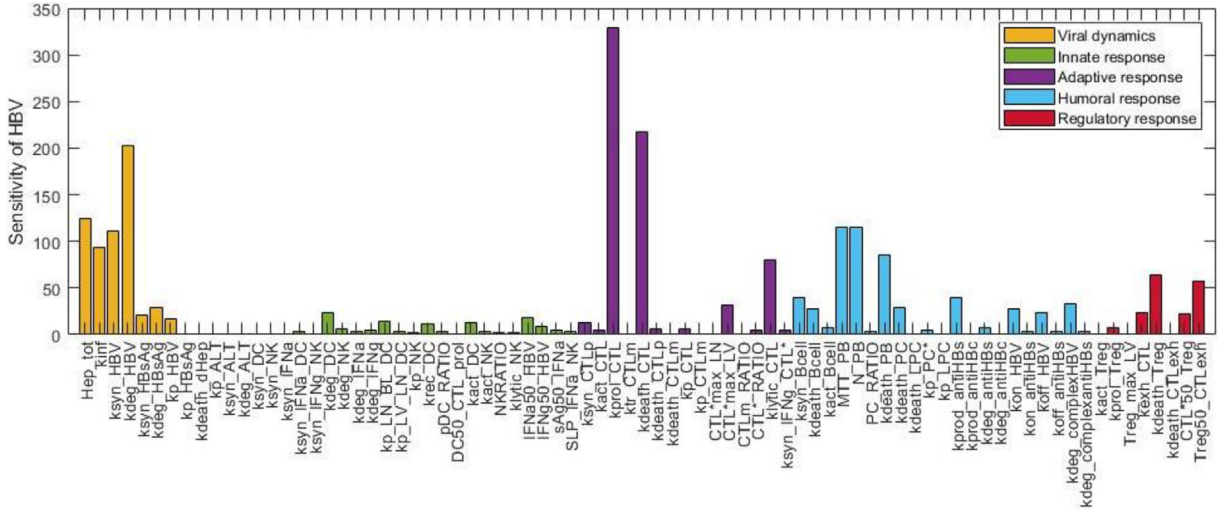

Fig. 4. Local sensitivity analysis. Sensitivity index for the different model parameters grouped by immune pathway computed as the integral of the fully normalized sensitivity profiles over HBV DNA time profiles. Parameters defined within the text and in Supplementary Table 1.

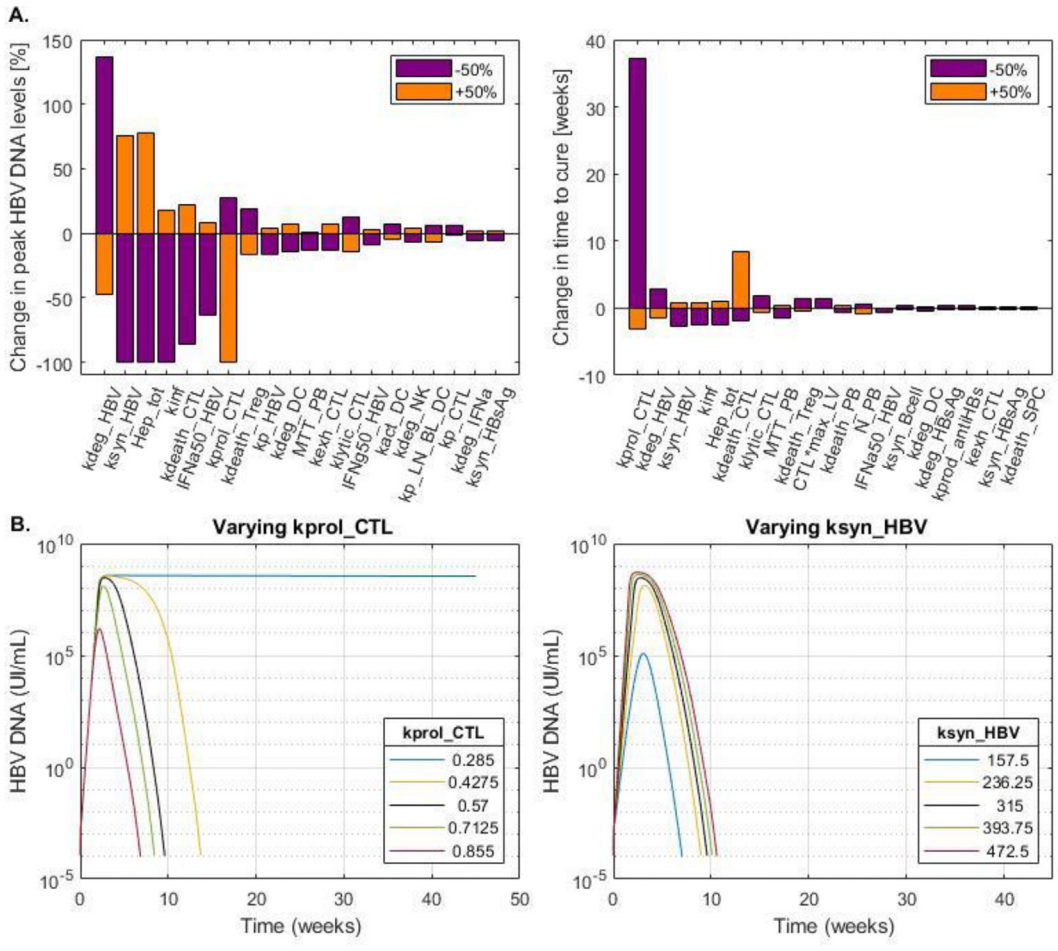

Fig. 5. Parameter scan analysis. A) Impact of 50% change on peak HBV DNA levels or time to cure (defined as HBV DNA < 20 IU/L & maximum simulation time of 45 weeks) when varying one parameter at a time. B) Impact of varying CTL proliferation rate constant (kprol_CTL) or HBV synthesis constant (ksyn_HBV) on the time course of circulating DNA viral levels (HBV DNA). Parameters defined within the text and in Supplementary Table 1.

Consistent with the parameter analyses results, blocking the activation of NK cells had no impact on viral dynamics or course. Similarly, blocking B cell activation or increasing the inhibitory effects of regulatory T cells by a factor of 5 had some impact on slowing down the elimination of antigen or delaying the start of viral clearance respectively, but

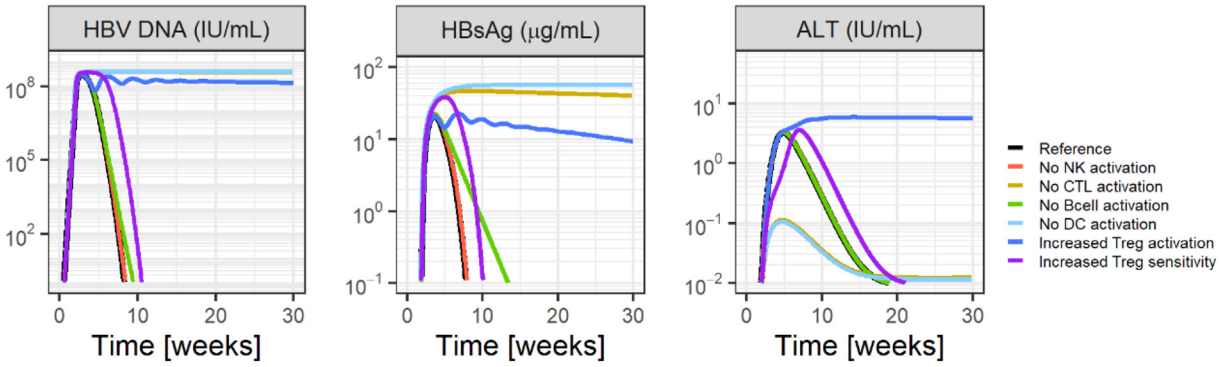

Fig. 6. Knock-out analysis. Model predicted time course of viral load (HBV DNA), surface hepatitis B antigen (HBsAg), and alanine aminotransferase (ALT) in blood under different knock-out scenarios: no perturbation (reference), no NK activation ($k_{act\_NK} = 0$), no CTL activation ($k_{act\_CTL} = 0$), no Bcell activation ($k_{act\_BcelI} = 0$), no DC activation ($k_{act\_DC} = 0$), increased Treg activation ($CTL_{50\_Treg\_prol} = 200000$) or increased Treg sensitivity to CTL exhaustion ($Treg_{50\_CTL\_exh} = 200000$). Entities defined within the text.

did not change the ultimate outcome, AHB disease resolution.

On the other hand, when blocking the activation of effector cells (CTL) or the antigen presentation to DC to initiate the response, an outcome of CHB scenario was predicted. A similar outcome was observed when the sensitivity to the activation of the immunoregulatory response was increased by a factor of 5, although with a sustained hepatic damage trigger by the remaining CTLs.

3.3.2. Chronicity

To further explore the captured behaviour described under model evaluation, the capability of the model to predict self-resolution or evolution to a chronic status was evaluated at a population level. Those parameters exhibiting higher impact on the sensitivity analysis – 11 in total- were selected and varied to simulate a virtual population: viral infectivity (k_{inf}), replication (k_{syn_HBV}) and degradation (k_{deg_HBV}) rate constants representing viral dynamics; CTL proliferation (k_{prol_CTL}), degradation (k_{deg_CTL}) and lytic activity (k_{lytic_CTL}) rate constants representing the cellular adaptive response; PB death rate constant (k_{death_PB}), PB mean transit time (MTT_{PB}), and number of transit compartments (NN_{PB}) regarding the humoral response; and Treg death rate (k_{death_Treg}) and Treg levels triggering 50% of maximum rate of CTL exhaustion ($Treg_{50\_CTLexh}$) representing the immunoregulatory response. The maximum (total) number of hepatocytes was not varied, as it rather represents a physiological parameter, which can be considered constant. In addition, no parameters regarding the innate response were selected due to their limited impact.

The virtual simulated population provided a simulated percentage of chronicity of 4.6 % with a 95% confidence interval of 3.0–6.4 %. Supplementary Fig. 2 shows the distribution of simulated parameters for the population of patients with acute and chronic disease. Major differences were seen in parameters accounting for CTL proliferation and CTL degradation.

4. Discussion

Different mathematical models have been developed previously for acute HBV; however, they have focused on certain aspects of the immune response in isolation. To our knowledge, this is the first quantitative systems pharmacology (QSP) model that aims to integrate in a single framework the role of different relevant immune response components -innate, adaptive and immunoregulatory – involved in HBV viral clearance, across multiple compartments (plasma, liver, and lymph nodes).

To build the final QSP model, information from multiple sources including existing models, clinical quantitative knowledge, and in vitro experiments have been integrated. While the model scope was mainly orientated to human data, there are certain biological aspects, such as B cell response, that have only been evaluated in animal species due to the limited ability to study them in humans or using in vitro human models [13]. In these situations, the use of data from animal models was necessary, representing an unavoidable model limitation. Once additional knowledge is gathered in humans, especially understanding host and viral interactions in the liver, that information will be helpful to optimize the model.

The course of HBV infection can be extremely variable depending on a wide range of viral and host factors such as the size of the inoculum or the route of infection, among others [36]. However, with a minimum inoculum size (1000 copies of HBV DNA) mimicking the inoculum of a needle [38], the proposed model was capable of successfully reproducing the typical time course of AHB from a qualitative and quantitative point in view [36,39]. In this regard, the model predicted HBV DNA to be the first viral marker appearing in blood with levels remaining above 240 IU/mL for 7 weeks, and a predicted time from peak to negativity (20 IU/mL) of 55 days, consistent with previous knowledge [40,41]. HBV DNA levels were then followed by an increase in HBsAg with a predicted antigenemia length of 60 days, close to the 56 days reported by Yoshikawa et al. [41]. Both of those biomarkers are predicted to appear, before the increase in ALT levels, which peaked 2 weeks after maximum levels of HBV DNA [36,39]. Nonetheless, time from infection to peak HBV DNA was underpredicted by the model, 3 weeks versus 6–8 weeks previously reported by Schmidt et al. [42], suggesting that there is an initial latency period during which the virus does not replicate or has a very low (undetectable) replication.

In addition to the known time course of the disease, the model was able to accurately capture the temporal profiles from patients followed during the acute disease (in the absence of treatment). This aspect highlights model validity, especially since only ALT levels were used to estimate release rate and the rest of the clinical data were directly used to validate model performance. Regarding the appearance of HBV-specific antibodies, quantitative data to support different synthesis processes were not available in the literature. However, due to the high affinity of anti-HBs to both viral particles and HBsAg subviral particles, their levels were not predicted to rise above the quantification threshold until viral clearance. This mimics the known early appearance of anti-HBc, and rise of anti-HBs late in infection and during the recovery [39]. The successful results from the model evaluation indicate that the different elements of the model are well aligned, and the parameter values were adequately selected, derived, or fine-tuned.

The holistic nature of the developed model enables us to explore *in silico* the relative contribution of the different arms of the immune response to the ultimate viral clearance. In agreement with general knowledge [16], the innate response had no or negligible impact on viral clearance. Interestingly, the model did not assume a "stealth virus", so HBV could be sensed and initiate an antiviral innate response (i.e., activation of NK cells and synthesis of IFNα) [16]. This response was limited by subviral particles (i.e., HBsAg) that can inhibit IFNα synthesis [10,43], and thus also the subsequent expression of interferon stimulated genes (ISG), which indeed do not appear to be activated during the early phase [43-57]. Regarding the humoral response, the model predicted some impact, especially during late viral clearance, supporting a role in controlling viral levels in the long term [13]. However, its suppression did not change the ultimate outcome of the disease during acute scenarios. The only factor predicted as essential for viral clearance was the presence of a HBV-specific CD8+ T cell response [16,47]. This was also experimentally shown when depletion of CD8+ T cells in chimpanzees led to HBV chronicity [48].

Among the different processes involved in CD8+ response, proliferation and death of CTLs seemed to explain better the HBV profiles than their cytotoxic and non-cytotoxic triggered processes. Indeed, univariate moderate changes in CTL proliferation were sufficient to trigger a chronic status. This is in agreement with clinical observations that patients with CHB tend to have weaker CTL response compared with those with AHB [49,50]. Unfortunately, T cell response in chronically infected patients is poorly understood. Different mechanisms such as T cell depletion, exhaustion, or T cell dysfunction have been proposed [47]. In our modelling framework, increasing the activation of regulatory T cells was shown to also lead to a chronic status. Although regulatory T cells (and presumably MDSC) may contribute to this T cell suppression [14,51], whether the functional exhaustion of HBV-specific CD8+ T cells is the sole or dominant contributor to CD8+ T cell failure, or whether the virus can also escape through the generation of viral escape sequence variants, like in HIV and HCV infection, and/or evasion mechanisms triggered by HBsAg [52] are currently open questions under extensive research, and therefore not incorporated in the model at this stage.

When the parameter scan was applied to a theoretical chronic scenario triggered by an increased immunoregulatory response to investigate what processes were most meaningful, the impact of the CTL proliferation parameter on viral levels was negligible, while blocking viral infectivity or synthesis could decrease viral load below detectable thresholds (both provided comparable results; Supplementary Fig. 3). In addition, increasing the lytic capability of CTLs or acting on the immunoregulatory stimulus could also suppress viral levels (data not shown).

Naturally, this model development presents some limitations. Quantitative human data to support all model processes were not always available and some parameters had to be derived from animal data (e.g., humoral response) or calibrated. In this regard, this QSP framework can be seen as an opportunity to better understand differences in the disease between animals and humans enabling its use to characterize longitudinal data from other species [48]. When additional animal and human data become available, the model can be expanded for use in translational research and drug development applications.

Additionally, knowledge in HBV is fast evolving. Therefore, there are other biological aspects of the host-immune interaction, such as the potential role of HBeAg or HBV X protein (HBx) on the development of a tolerance status [47,53,54], or the emerging interest in myeloid derived suppressor cells for their capability to also induce T cell exhaustion [55] and Treg expansion [56], which are either not well characterized from a quantitative perspective or for which contradictory results are available. These processes are likely to be of limited relevance in AHB, and consequently they have not been incorporated into the current model. However, as new quantitative data emerges and additional knowledge is acquired and confirmed, the mechanistic nature of the model might enable its extension to include additional mechanisms to refine and improve its usefulness in HBV infection. The current model did not evaluate the impact of HBV genotypes and mutations on viral dynamics [57]. Results from the sensitivity analysis revealed that parameters representing viral dynamics did show an impact on HBV DNA levels but did not impact the transition from acute to chronic status. However, those results should not be applied more broadly without further investigation.

Despite these limitations, when simulating a virtual population that takes into account reasonable variability (30%) on the most influential model parameters and using the modeling framework developed for the acute scenario, development of chronic HBV infection was predicted for 4.6% of the simulated population. This observation is in line with epidemiological data that estimate that 5% of patients evolve to chronic HBV infection after horizontal transmission of the disease [2] and supports the robustness and validity of the proposed model structure for viral hepatitis, especially considering that the virtual population was not previously calibrated selecting only subsets of simulated patients, and that development of chronicity is one of the most relevant outcomes from the proposed model.

Some of the natural future applications of the current model in acute HBV infection are: (i) predicting HBV-related acute liver failure, (ii) predicting response to acute HBV infection therapies, and (iii) exploring differences in both treatment response and progression of the acute disease for patients with HBV, including those with pre-existing liver disease (e.g., NAFLD/NASH). Dedicated literature searches and model building would be needed to adapt the current model for these purposes.

5. Conclusions

In summary, a QSP model that integrates in a quantitative framework the widely accepted biological processes triggered upon AHB infection has been developed and successfully applied to clinical data. Additional studies performed not only in peripheral blood, but also at the liver environment are required to better understand the complex host-virus interactions that govern the ultimate outcome in HBV infection, especially regarding the interplay between viral components, and host adaptive and regulatory immune responses. In this regard, this QSP model provides a valuable tool to identify knowledge gaps and validate hypotheses. Moreover, given the mechanistic nature of the framework, it can easily accommodate new knowledge in this highly dynamic field, as well as serve as basis to integrate different potential mechanisms of response.

6. Summary declaration of interest

At the time the research was performed, EASP, ZPPG, JDGM and IFT received research funding from Janssen Research & Development; no grant number is applicable. JV, KS, XWT, and JJPR are employed by Janssen Pharmaceuticals.

CRediT authorship contribution statement

Eduardo Asín-Prieto: Methodology, Formal analysis, Validation, Writing - original draft. **Zinnia P. Parra-Guillen:** Methodology, Formal analysis, Validation, Writing - original draft. **José David Gómez Mantilla:** Methodology, Formal analysis, Validation, Writing - original draft. **Joris Vandenbossche:** Conceptualization,

Supervision, Project administration. **Kim Stuyckens:** Writing - review & editing. **Xavier Woot de Trixhe:** Writing - review & editing. **Juan José Perez-Ruixo:** Conceptualization, Writing - review & editing, Supervision, Funding acquisition. **Iñaki F. Troconiz:** Conceptualization, Writing - original draft, Supervision.

Declaration of Competing Interest

The authors declare that they have no known competing financial interests or personal relationships that could have appeared to influence the work reported in this paper.

Acknowledgments

Technical editorial assistance was provided by Kimberly Dittmar, PhD, of Cello Health Communications/MedErgy, and was funded by Janssen Global Services, LLC.

Appendix A. Supplementary data

Supplementary data to this article can be found online at https://doi.org/10.1016/j.csbj.2021.08.052.

References

[1] Tang LSY, Covert E, Wilson E, Kottilil S. Chronic hepatitis B infection. JAMA 2018;319(17):1802. https://doi.org/10.1001/jama.2018.3795.
[2] World Health Organization. (2018) Hepatitis B – Fact sheet Available from: https://www.who.int/en/news-room/fact-sheets/detail/hepatitis-b.
[3] Lok AS, Zoulim F, Dusheiko G, Ghany MG. Hepatitis B cure: from discovery to regulatory approval. Hepatology 2017;66(4):1296–313.
[4] Terrault NA, Lok ASF, McMahon BJ, Chang K-M, Hwang JP, Jonas MM, et al. Update on prevention, diagnosis, and treatment of chronic hepatitis B: AASLD 2018 hepatitis B guidance. Hepatology 2018;67(4):1560–99.
[5] Al-Mahtab M, Bazinet M, Vaillant A, Su C-W. Safety and efficacy of nucleic acid polymers in monotherapy and combined with immunotherapy in treatment-naive Bangladeshi patients with HBeAg+ chronic hepatitis B infection. PLoS ONE 2016;11(6):e0156667. https://doi.org/10.1371/journal.pone.0156667.
[6] Bazinet M, Pântea V, Placinta G, Moscalu I, Cebotarescu V, et al. Safety and efficacy of 48 weeks REP 2139 or REP 2165, tenofovir disoproxil, and pegylated interferon Alfa-2a in patients with chronic HBV infection NaIve to Nucleos(t)ide Therapy. Gastroenterology 2020;158:2180–94.
[7] Vanwolleghem T, Hou J, van Oord G, Andeweg AC, Osterhaus ADME, Pas SD, et al. Re-evaluation of hepatitis B virus clinical phases by systems biology identifies unappreciated roles for the innate immune response and B cells. Hepatology 2015;62(1):87–100.
[8] Liu HY, Zhang XY. Innate immune recognition of hepatitis B virus. World J Hepatol. 2015;7(21):2319–22.
[9] Tjwa ETTL, van Oord GW, Hegmans JP, Janssen HLA, Woltman AM. Viral load reduction improves activation and function of natural killer cells in patients with chronic hepatitis B. J Hepatol 2011;54(2):209–18.
[10] Xu Y, Hu Y, Shi B, Zhang X, Wang J, Zhang Z, et al. HBsAg inhibits TLR9-mediated activation and IFN-α production in plasmacytoid dendritic cells. Mol Immunol 2009;46(13):2640–6.
[11] Guidotti LG, Ishikawa T, Hobbs MV, Matzke B, Schreiber R, Chisari FV. Intracellular inactivation of the hepatitis B virus by cytotoxic T lymphocytes. Immunity 1996;4(1):25–36.
[12] Schuch A, Hoh A, Thimme R. The Role of Natural Killer Cells and CD8+ T Cells in Hepatitis B Virus Infection. Front Immunol 2014;5:1–8.
[13] Zhang S, Zhao J, Zhang Z. Humoral immunity, the underestimated player in hepatitis B. Cell Mol Immunol 2018;15(6):645–8.
[14] Stoop JN, van der Molen RG, Baan CC, van der Laan LJW, Kuipers EJ, Kusters JG, et al. Regulatory T cells contribute to the impaired immune response in patients with chronic hepatitis B virus infection. Hepatology 2005;41(4):771–8.
[15] Xu D, Fu J, Jin L, Zhang H, Zhou C, Zou Z, et al. Circulating and liver resident CD4+CD25+ regulatory T Cells actively influence the antiviral immune response and disease progression in patients with hepatitis B. J Immunol 2006;177(1):739–47.
[16] Boeijen LL, Hoogeveen RC, Boonstra A, Lauer GM. Hepatitis B virus infection and the immune response: the big questions. Best Pract Res Clin Gastroenterol 2017;31(3):265–72.
[17] Nowak MA, Bonhoeffer S, Hill AM, Boehme R, Thomas HC, McDade H. Viral dynamics in hepatitis B virus infection. Proc Natl Acad Sci USA 1996;93(9):4398–402.
[18] Ciupe SM, Ribeiro RM, Nelson PW, Dusheiko G, Perelson AS. The role of cells refractory to productive infection in acute hepatitis B viral dynamics. Proc Natl Acad Sci USA 2007;104(12):5050–5.
[19] Ciupe SM, Ribeiro RM, Nelson PW, Perelson AS. Modeling the mechanisms of acute hepatitis B virus infection. J Theor Biol 2007;247(1):23–35.
[20] Ciupe SM, Ribeiro RM, Perelson AS, Regoes RR. Antibody responses during hepatitis B viral infection. PLoS Comput Biol 2014;10(7):e1003730. https://doi.org/10.1371/journal.pcbi.1003730.
[21] Ciupe SM, Hews S. Mathematical models of e-antigen mediated immune tolerance and activation following prenatal HBV infection. PLoS ONE 2012;7(7):e39591.
[22] Fatehi Chenar F, Kyrychko YN, Blyuss KB. Mathematical model of immune response to hepatitis B. J Theor Biol 2018;447:98–110.
[23] Forde J, Ciupe S, Cintron-Arias A, Lenhart S. Optimal control of drug therapy in a hepatitis B model. Appl Sci 2016;6(8):219.
[24] Yousfi N, Hattaf K, Tridane A. Modeling the adaptive immune response in HBV infection. J Math Biol 2011;63(5):933–57.
[25] Marchuk GI, Petrov RV, Romanyukha AA, Bocharov GA. Mathematical model of antiviral immune response. I. Data analysis, generalized picture construction and parameters evaluation for hepatitis B. J Theor Biol 1991;151(1):1–40.
[26] Palsson S, Hickling TP, Bradshaw-Pierce EL, Zager M, Jooss K, O'Brien PJ, et al. The development of a fully-integrated immune response model (FIRM) simulator of the immune response through integration of multiple subset models. BMC Syst Biol 2013;7(1):95. https://doi.org/10.1186/1752-0509-7-95.
[27] Asín-Prieto E, Parra-Guillen ZP, Mantilla JDG, Vandenbossche J, Stuyckens K, de Trixhe XW, et al. Immune network for viral hepatitis B: Topological representation. Eur J Pharm Sci 2019;136:104939. https://doi.org/10.1016/j.ejps.2019.05.017.
[28] Herman IP. Terminology, the standard human, and scaling physics of the human body. In: Physics of the Human Body. Berlin: Springer; 2007. p. 1–36.
[29] Sharma R, Sharma S. Physiology, Blood Volume In: StatPearls. Treasure Island (FL): StatPearls Publishing; 2019.
[30] Prothero JW. Organ scaling in mammals: the liver. Comp Biochem Physiol Part A Physiol 1982;71(4):567–77.
[31] Kim HY, Kwon H-D, Jang TS, Lim J, Lee H-S, Takehara T. Mathematical modeling of triphasic viral dynamics in patients with HBeAg-positive chronic hepatitis B showing response to 24-week clevudine therapy. PLoS ONE 2012;7(11):e50377. https://doi.org/10.1371/journal.pone.0050377.
[32] Balbas-Martinez V, Asin-Prieto E, Parra-Guillen ZP, Troconiz IF. A quantitative systems pharmacology model for the key interleukins involved in Crohn's disease. J Pharmacol Exp Ther. 2020;372(3):299–307.
[33] Kan QC, Li DL, Yu ZJ. Vector-mediated expression of interferon gamma inhibits replication of hepatitis B virus in vitro. Acta Virol 2013;57(04):421–728.
[34] Kan Q, Li D, Yu Z. Specific expression of human interferon-gamma controls hepatitis B virus replication in vitro in secreting hepatitis B surface antigen hepatocytes. J Virol Methods 2012;180(1-2):84–90.
[35] Phillips S, Chokshi S, Riva A, Evans A, Williams R, Naoumov NV. CD8 + T cell control of hepatitis B virus replication: direct comparison between cytolytic and noncytolytic functions. J Immunol 2010;184(1):287–95.
[36] Hollinger FB. Hepatitis B virus infection and transfusion medicine: science and the occult. Transfusion 2008;48(5):1001–26.
[37] Chulanov VP, Shipulin GA, Schaefer S, Gerlich WH. Kinetics of HBV DNA and HBsAg in acute hepatitis B patients with and without coinfection by other hepatitis viruses. J Med Virol 2003;69(3):313–23. https://doi.org/10.1002/jmv.10291.
[38] Whalley SA, Murray JM, Brown D, Webster GJM, Emery VC, et al. Kinetics of acute hepatitis B virus infection in humans. J Exp Med 2001;193(7):847–853.
[39] Liang TJ. Hepatitis B: the virus and disease. Hepatology 2009;49(5 Suppl):S13–21.
[40] Yoshikawa A, Gotanda Y, Itabashi M, Minegishi K, Kanemitsu K, Nishioka K. Hepatitis B NAT virus-positive blood donors in the early and late stages of HBV infection: analyses of the window period and kinetics of HBV DNA. Vox Sang 2005;88(2):77–86.
[41] Yoshikawa A, Gotanda Y, Minegishi K, Taira R, Hino S, Tadokoro K, et al. Lengths of hepatitis B viremia and antigenemia in blood donors: preliminary evidence of occult (hepatitis B surface antigen-negative) infection in the acute stage. Transfusion 2007;47(7):1162–71.
[42] Schmidt J, Blum HE, Thimme R. T-cell responses in hepatitis B and C virus infection: similarities and differences. Emerg Microbes Infect 2013;2(1):1–8.
[43] Woltman AM, Op den Brouw ML, Biesta PJ, Shi CC, Janssen HLA, Wedemeyer H. Hepatitis B virus lacks immune activating capacity, but actively inhibits plasmacytoid dendritic cell function. PLoS ONE 2011;6(1):e15324. https://doi.org/10.1371/journal.pone.0015324.
[44] Wieland S, Thimme R, Purcell RH, Chisari FV. Genomic analysis of the host response to hepatitis B virus infection. Proc Natl Acad Sci USA 2004;101(17):6669–74.
[45] Fisicaro P, Valdatta C, Boni C, Massari M, Mori C, Zerbini A, et al. Early kinetics of innate and adaptive immune responses during hepatitis B virus infection. Gut 2009;58(7):974–82.
[46] Dunn C, Peppa D, Khanna P, Nebbia G, Jones M, Brendish N, et al. Temporal analysis of early immune responses in patients with acute hepatitis B virus infection. Gastroenterology 2009;137(4):1289–300.
[47] Baumert TF, Thimme R, von Weizsäcker F. Pathogenesis of hepatitis B virus infection. World J Gastroenterol 2007;13(1):82–90.
[48] Thimme R, Wieland S, Steiger C, Ghrayeb J, Reimann KA, Purcell RH, et al. CD8(+) T cells mediate viral clearance and disease pathogenesis during acute hepatitis B virus infection. J Virol 2003;77(1):68–76.

[49] Sobao Y, Tomiyama H, Sugi K, Tokunaga M, Ueno T, Saito S, et al. The role of hepatitis B virus-specific memory CD8 T cells in the control of viral replication. J Hepatol 2002;36(1):105–15.
[50] Hoogeveen RC, Robidoux MP, Schwarz T, Heydmann L, Cheney JA, Kvistad D, et al. Phenotype and function of HBV-specific T cells is determined by the targeted epitope in addition to the stage of infection. Gut 2019;68(5):893–904.
[51] Franzese O, Kennedy PTF, Gehring AJ, Gotto J, Williams R, Maini MK, et al. Modulation of the CD8 + -T-Cell response by CD4 + CD25 + regulatory T cells in patients with hepatitis B virus infection. J Virol 2005;79(6):3322–8.
[52] Faure-Dupuy S, Lucifora J, Durantel D. Interplay between the hepatitis B virus and innate immunity: From an understanding to the development of therapeutic concepts. Viruses 2017;9(5):95.
[53] Guidotti LG, Isogawa M, Chisari FV. Host-virus interactions in hepatitis B virus infection. Curr Opin Immunol 2015;36:61–6.
[54] Sartorius K, Swadling L, An P, Makarova J, Winkler C, Chuturgoon A, et al. The multiple roles of hepatitis B virus X protein (HBx) dysregulated microRNA in hepatitis B virus-associated hepatocellular carcinoma (HBV-HCC) and immune pathways. Viruses 2020;12(7):746. https://doi.org/10.3390/v12070746.
[55] Pallett LJ, Gill US, Quaglia A, Sinclair LV, Jover-Cobos M, Schurich A, et al. Metabolic regulation of hepatitis B immunopathology by myeloid-derived suppressor cells. Nat Med 2015;21(6):591–600.
[56] Kondo Y, Shimosegawa T. Significant roles of regulatory T cells and myeloid derived suppressor cells in hepatitis B virus persistent infection and hepatitis B Virus-Related HCCs. Int J Mol Sci 2015;16(2):3307–22.
[57] Caligiuri P, Cerruti R, Icardi G, Bruzzone B. Overview of hepatitis B virus mutations and their implications in the management of infection. World J Gastroenterol 2016;22(1):145–54.
[58] Webster GJ, Reignat S, Maini MK, Whalley SA, Ogg GS, et al. Incubation phase of acute hepatitis B in man: dynamic of cellular immune mechanisms. Hepatology 2000;32(5):1117–24.